

ASYMMETRICAL FAULT RIDE THROUGH AS ANCILLARY SERVICE BY CONSTANT POWER LOADS IN GRID-CONNECTED AREA

G.Navyasree¹, V.Syam Kumar²

¹M.Tech Student, Anu Bose Institute of Technology, Paloncha, khammam, Telangana, India

²Assoc Prof Dept of EEE, Anu Bose Institute of Technology, Paloncha, khammam, Telangana, India

Abstract—The introduction of distributed generation (DG) into low voltage (LV) systems demands that the generation system remain grid connected during voltage sags to ensure the operational stability. The DG consisting of fixed speed squirrel cage induction generator (SCIG)-based wind turbines is unable to provide reactive power control and needs a dedicated compensating device. Under asymmetrical grid faults the negative sequence flux circulation in the airgap introduces the torque oscillations that lead to the reduction of lifetime of the generation system. This paper proposes the use of distributed constant power loads (CPLs) for asymmetrical fault ride through (FRT) instead of using a centralized STATCOM. It has also been observed that the compensation of negative sequence voltage improves the performance of SCIG by eliminating the torque ripples. The compensation of positive sequence voltage avoids a possible voltage collapse at the LV distribution level and improves the reliability and stability of the wind farm. Centralized compensation of the asymmetrical grid fault by a STATCOM is compared with the distributed compensation by CPLs. The results suggest that each individual CPL injects lower current for maximum FRT enhancement compared to a dedicated STATCOM.

I. INTRODUCTION

DUE to the environment advantages and being close to the point of power utilization the use of renewable energy resources is rapidly growing at the distribution level. Among them, photovoltaic and wind turbines are gaining increasing attention

[1]. Power generation from wind energy and its integration to the local distribution grid is relatively newer approach

[2]. In the last decade, the technological developments have made it possible to change the generator types used for wind farm from fixed speed to variable speed concept. However, squirrel cage induction generator (SCIG)-based wind farms represent a considerable 30% of the installed wind power in Europe

[3] and enhancing their fault ride through (FRT) capability is indispensable in order to increase the power system stability and reliability. Additionally, for microhydro applications, SCIG is still the cost effective and reliable power generation source. To maintain the stability of the utility grid, grid operators have specified the requirements for the integration

of DERs. For wind power plants, the grid connection requirements demand FRT capability and reactive current injection in order to maintain the stability of the power system [6]–[10]. In UK, FRT capability requirements demand that terminal voltage of the wind farm not be less than 15% of the nominal voltage during the fault and it must be restored to 90% within 0.5 s. Grid codes in Denmark set the minimum voltage level during the fault to 25% of the nominal voltage and it should be restored to 75% within 0.75 s [6]–[8]. These grid codes requirements are independent of the type of compensators and can be achieved by using either active or passive compensators. In the case of SCIG-based wind farms, the absence of any power electronic (PE) compensating device does not allow FRT enhancement and reactive injection to fulfill the grid code requirements. Different methods have been investigated to fulfill the grid code requirements and enhance the FRT capability of a wind farm. These include the use of doubly fed induction generator (DFIG)-based wind farms for variable speed applications and a centralized STATCOM for fixed speed applications [11]–[19]. It has been observed that DFIG experiences inherent difficulties to ride through grid faults due to the high voltage induced in the rotor circuit. Many practical strategies of STATCOM reactive power control under asymmetrical grid faults and load unbalances have been discussed in [5] and [17] and proved to be very effective. However, the installation of a dedicated switching compensator or a STATCOM is not very cost effective. The rapidly changing modern power infrastructure can utilize some of its installed resources for the services that were earlier provided by the dedicated devices. PE load interface, when tightly regulated, draws a constant active power from the utility and behaves as a constant power load (CPL). It is adaptive to the fluctuations in the grid voltage at its terminal and always keeps the input power constant [20]–[29]. The number of this kind of load has been rapidly growing and will continue to increase in the near future. Battery charger for electric vehicles, motor drives and large rectifiers for DC loads are few examples of CPLs. The use of single CPL for FRT enhancement has been discussed in [29] as a starting point. The rapidly changing modern power infrastructure can utilize some of its installed resources for the services that were earlier provided by the dedicated devices. PE load interface, when tightly regulated, draws a constant active power from the

utility and behaves as a constant power load (CPL).using adistribution system model. The study, however no comparison of the current rating of the PE devices acting as CPLs with the existing STATCOM solution. The modern distribution systems have many CPLs distributed across the network and the proper utilization of these resources for ancillary grid services is more practical and beneficial to improve the efficiency and performance of the entire power system compared to the use of a single CPL reported in [29].

This paper proposes the application of tightly regulated PE load interfaces or CPLs, connected to fixed speed SCIG-based wind farm for FRT enhancement under asymmetrical grid faults. For variable speed applications, CPLs can help to reduce the current rating of the generation side converters on each wind turbine by sharing some of the ancillary services. In addition to the typical positive sequence reactive current injection, the proposed method suggests a negative sequence active and reactive current injection during the FRT operation to mitigate the voltage unbalances without exceeding the peak current limit of the PE load interface. A comparison between the distributed compensation of active and reactive power by CPLs and the centralized compensation by a STATCOM indicates a lower per unit current rating for each distributed PE device compared to the centralized compensation solution offered by STATCOM.

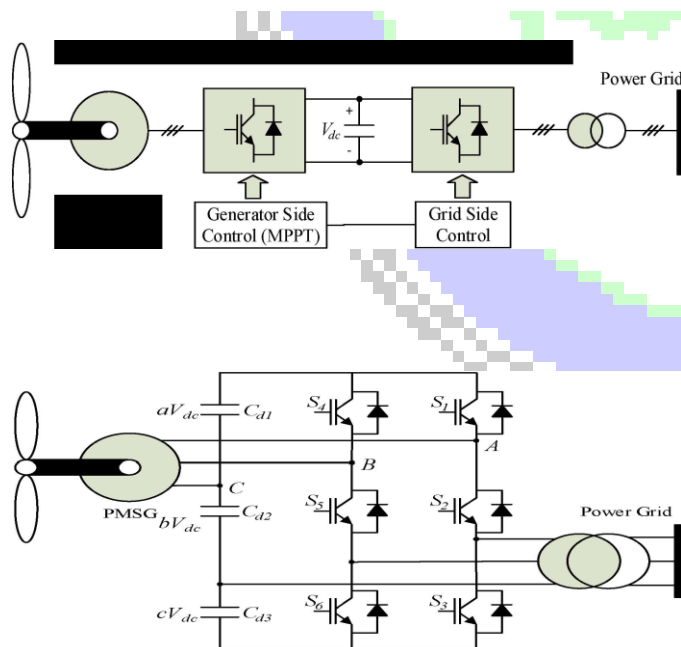


Figure 2. Variabe speed wind energy systems based on six switch ACIAC converter

II. CPL AND NEGATIVE RESISTANCE

CPL is usually an active rectifier such as three-phase full-bridge inverter with IGBTs or other similar switching semiconductor devices. Three-phase diode and thyristor front end rectifiers can be used as CPL but they do not provide much control flexibility. An active rectifier provides more flexibility in operation, power factor controllability and reduced THD. A well-known application of an active rectifier is a voltage source converter (VSC) as it is naturally suited for controlling active and reactive current in a decoupled manner using vector control principles [30]. In this way, the inverter can control the direct current component absorbed toward the load independently of the control of reactive current, which can be injected toward the grid, thus supporting the stability of the power system under abnormal grid voltage conditions. Fig. 1 illustrates the simplified model of a CPL.

III. OBSERVER BASED ESTIMATION SYSTEM

A. Observer Method Principles

In practice, not all state variables are measured. The reasons are that this is not physically feasible or that the sensors required are probably too expensive. For this reason it is needed to demonstrate how to reconstruct the complete state information based on the measured output y . The assumption is that we know the system description (A,B,C) and that (A,C) is observable [11].

One method of estimating the state x in an observer is to construct a full order model of the plant dynamics

$$\dot{\hat{x}} = A\hat{x} + Bu \quad (3)$$

Where \hat{x} is the estimate of the actual state x and A , B and u are known. If this observer can be started with the correct initial condition $\hat{x}(0) = x(0)$, it will always deliver $\hat{x}(t) = x(t)$. However, it is precisely the lack of information about $x(0)$ that requires the construction of an observer. The effect of an error in the initial condition \hat{x} can be studied by defining the estimation error, $\tilde{x} = x - \hat{x}$.

$$\dot{\tilde{x}} = A\tilde{x} + Bu \quad (4)$$

$$\dot{\tilde{x}} - \dot{\hat{x}} = A(\tilde{x} - \hat{x}) \quad (5)$$

$$\dot{\tilde{x}} = A\tilde{x} \quad (6)$$

The dynamics of \tilde{x} are described by the system matrix A . If it is unstable, then the estimation error diverges. If A is stable then \tilde{x} converges towards zero — however, probably very slowly. Furthermore, effects like noise or errors in the system description (A,B) might cause the estimate to diverge from the true state.

The feedback in the observer is introduced to enforce stability of the error dynamics and/or for faster convergence. The difference between the measured and the estimated outputs are used to correct the estimated state, see Fig. 5.

The equation for this scheme is

$$\dot{\hat{x}} = A\hat{x} + Bu + H(y - C\hat{x}) \quad (7)$$

$$\dot{\tilde{x}} = (A - HC)\tilde{x} + Bu + HCx \quad (8)$$

resulting in the error dynamics

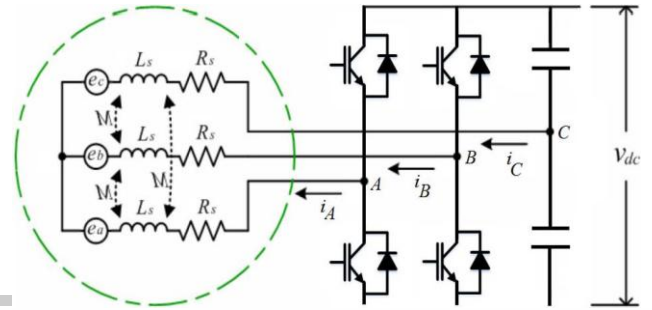
$$\dot{\tilde{x}} = (A - HC)\tilde{x} \quad (9)$$

If H is chosen such that the eigenvalues of (A - HC) have negative real parts then \tilde{x} will converge towards zero.

B. Modeling of Permanent Magnet Generator

The equivalent circuit of PMSG is shown in Fig. 6. Assuming that the stator resistances of all the windings are equal to zero and also self and mutual inductances are constant, the voltage equation of the three phases can be expressed as (10). In this equation, magnets, stainless steel retaining sleeves with high resistivity, and rotor-induced currents are neglected and no damper windings are modeled [12].

$$\begin{bmatrix} v_a \\ v_b \\ v_c \end{bmatrix} = \begin{bmatrix} R_s & 0 & 0 \\ 0 & R_s & 0 \\ 0 & 0 & R_s \end{bmatrix} \begin{bmatrix} i_a \\ i_b \\ i_c \end{bmatrix} + \begin{bmatrix} L_s - M & 0 & 0 \\ 0 & L_s - M & 0 \\ 0 & 0 & L_s - M \end{bmatrix} \frac{d}{dt} \begin{bmatrix} i_a \\ i_b \\ i_c \end{bmatrix} + \begin{bmatrix} e_a \\ e_b \\ e_c \end{bmatrix} \quad (10)$$



where v_a , v_b , and v_c are phase voltages. R_s , L_s and M are stator resistance, stator inductance and mutual inductance, respectively. i_a , i_b , and i_c are phase currents and e_a , e_b , and e_c are phase back-EMFs. Since the neutral point of PMSG is not offered, it is difficult to construct the equation for one phase. Therefore, the unknown input observer is considered by the following line-to-line equation:

$$\frac{di_{ab}}{dt} = -\frac{R_s}{L_s}i_{ab} + \frac{1}{L}v_{ab} - \frac{1}{L}e_{ab} \quad (11)$$

C. Proposed Sensorless Control System

In (11), i_{ab} and v_{ab} can be measured, therefore they are "known" state variables. On the other hand, since e_{ab} cannot be measured, this term is considered as an "unknown" state. The equation (11) can be rewritten in the following matrix form:

$$\dot{x} = Ax + Bu + Fw \quad (12)$$

$$y = Cx \quad (13)$$

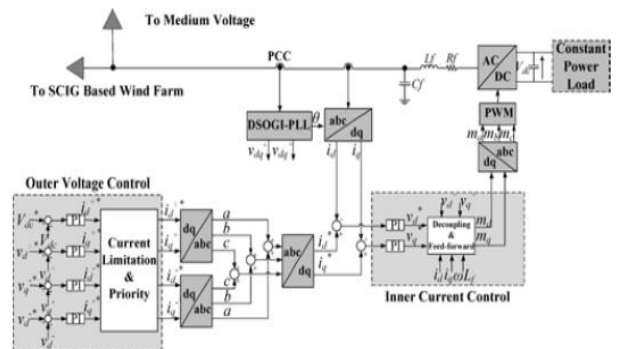
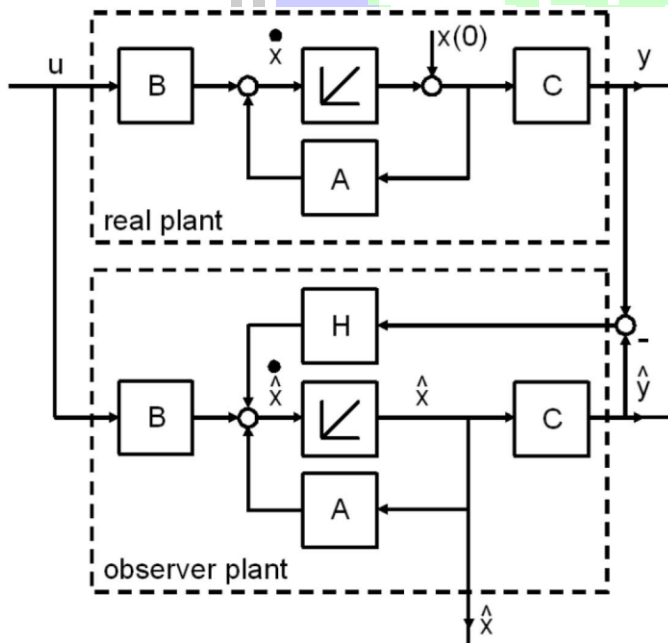


Fig. 2. CPL control structure with independent control of positive and negative sequence voltages at PCC.

H is the gain matrix of the observer in Fig. 5. As it was mentioned before, if H is selected properly, this observer can accurately estimate line to line currents and back-EMFs of PMSG and \tilde{i}_{ab} and \tilde{e}_{ab} will converge towards zero.

Therefore, the equation of whole observer including all of three phases is as follows:

$$\frac{d}{dt} \begin{bmatrix} \hat{i}_{ab} \\ \hat{e}_{ab} \end{bmatrix} = \begin{bmatrix} -\frac{R_s}{L} & -\frac{1}{L} \\ 0 & 0 \end{bmatrix} \begin{bmatrix} \hat{i}_{ab} \\ \hat{e}_{ab} \end{bmatrix} + \begin{bmatrix} 1 \\ L \end{bmatrix} v_{ab} + \begin{bmatrix} h_1 \\ h_2 \end{bmatrix} (i_{ab} - \hat{i}_{ab}) \quad (21)$$

Fig. 7 shows a block diagram of the proposed back-EMF observer system. Similarly we can calculate e_{bc} and e_{ca} and then from following equation the generator mechanical speed (ω_m) can be measured:

$$E = \max(E_{ab}, E_{bc}, E_{ca}) = 2P\lambda\omega_m \quad (22)$$

where E_{ab} , E_{bc} and E_{ca} are amplitudes of e_{ab} , e_{bc} and e_{ca} and P and λ are pole pairs and Flux linkage established by magnets, respectively.

Figure 7. Block diagram of the proposed back-EMF observer system

IV. CONTROL SYSTEM

Two independent control strategies are utilized for two three phase terminals of the proposed system, which are shown in Figs. 8 and 9. The control system consists of three parts: 1) Control of power delivered to the grid, 2) Vector control for PMSG and 3) sensorless MPPT. These control parts eventually produce V_{ref1} & V_{ref2} of PWM scheme for six-switch AC/AC converter switching.

A. Control of Power Delivered to the Grid

The control of grid side three phase terminal of six switch converter is achieved through DQ current control method. According to [7], active and reactive power control injected to the grid can be achieved by controlling direct current (i_d) and quadrature current (i_q) components, respectively. In fact, when the reference frame is oriented along the grid voltage, v_q will be equal to zero and hence active and reactive power can be expressed as

$$P = \frac{3}{2} V_d i_d \quad (23)$$

$$Q = \frac{3}{2} V_d i_q \quad (24)$$

As it can be seen in Fig. 8, DC voltage is also set by controlling active power through i_d control loop (Fig. 8)

B. Sequence Separation

The positive and negative sequence detection technique named as DSOGI-PLL translates the three-phase voltage from the abc to stationary $\alpha\beta$ reference frames [34]–[38]. DSOGI-based quadrature signals generator (QSG) is employed for filtering and obtaining the 90° shifted versions from the $\alpha\beta$ voltages. The QSG output signals act as inputs to the positive and negative sequence calculator (PNSC) [34]–[37]. The positive and negative sequence $\alpha\beta$ voltages are then transformed to the rotating SRF, such that

$$\begin{aligned} v_{dq}^+ &= [T_{dq}^+] v_{\alpha\beta}^+ = \begin{bmatrix} \cos \theta & \sin \theta \\ -\sin \theta & \cos \theta \end{bmatrix} v_{\alpha\beta}^+ \\ v_{dq}^- &= [T_{dq}^-] v_{\alpha\beta}^- = \begin{bmatrix} \cos \theta & -\sin \theta \\ \sin \theta & \cos \theta \end{bmatrix} v_{\alpha\beta}^- \end{aligned} \quad (12)$$

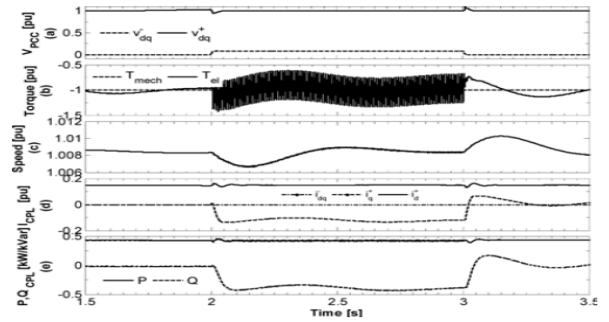


Fig. 7. Simulation results for positive sequence voltage control: (a) PCC voltages, (b) SCIG torque, (c) SCIG speed, (d) CPL₁ compensation currents, and (e) CPL₁ powers.

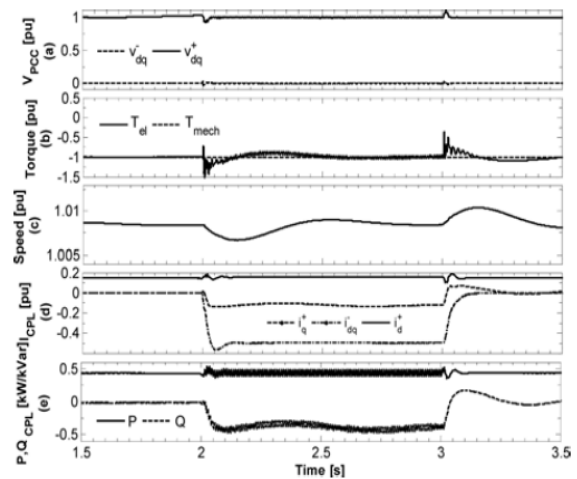


Fig. 9. Simulation results with coordinated positive and negative sequence voltage control: (a) PCC voltages, (b) SCIG torque, (c) SCIG speed, (d) CPL₁ compensation currents, and (e) CPL₁ powers.

SCIG consumes more reactive power from the grid, resulting in a continuous decrease in the positive sequence voltage component and eventually the voltage collapses. The system reaches the mechanical unstable point and cannot return to the rated operating point after the fault. Fig 8(e) shows the oscillating CPL active and reactive powers during the fault. In this case, the active and reactive powers can be represented by

$$\begin{aligned} P_{CPL} &= v_d^+ i_d^+ + v_d^- i_d^- + v_q^- i_q^- + v_d^- i_d^+ + v_d^+ i_d^- \\ Q_{CPL} &= v_d^- i_q^- - v_q^- i_d^- - v_q^- i_d^+ - v_d^+ i_q^- \end{aligned} \quad (21)$$

During the fault, both the active and reactive powers exhibit second-order harmonics as a result of interaction between the opposite sequence voltage and current components. The input active power oscillates around a constant load demand. The power oscillations under fault condition are higher in this case as confirmed by (21) compared to the previously discussed two cases.

D. CPLs With Coordinated Positive and Negative Sequence Voltage Control In this case, CPL control is allowed to compensate for both the positive and negative sequence voltage components independently under the same fault conditions. The results are illustrated in Fig. 9. Each CPL injects both the positive and negative sequence of the current for compensation purpose without exceeding its nominal current. The CPL control effectively compensates the positive and negative sequence voltages during the fault. It can also be observed that coordinated voltage control results in the substantial reduction of torque ripples and the acceleration of the rotor during the fault is avoided. SCIG regain power relationship is represented by (17) because all the positive and negative sequence voltage and current components are present in this case.

Simulation results enhance the understanding of the operation of SCIG-based wind farm when CPLs are controlled to provide the positive and negative sequence voltage compensation independently. The positive sequence voltage compensation enhances the torque capability of the SCIG and avoids the acceleration of the rotor, while the negative sequence voltage compensation helps to improve the lifetime of the generator drive train by removing the torque ripples. This is a situation where built-in distribution system resources are able to provide the FRT ancillary service that was earlier supposed to be achieved with a dedicated STATCOM or DFIG-based wind farm arrangements. However, voltage compensation capability is totally dependent on the chosen current rating of the individual CPL. These devices have to be designed for a current rating that must be higher than the active component of current representing their load power requirements.

VIII. CONCLUSION

This paper explores the possibility of using distributed CPLs to mitigate the asymmetrical grid faults in a distribution system supplied by SCIG-based wind farm. The proposed system configuration provides an alternative to the conventional STATCOM and DFIG wind turbine by effectively controlling the installed resources at the distribution level. A detailed simulation analysis is carried out to understand the voltage control performed by distributed CPLs and the resulting operation of the SCIG under unbalanced grid fault. A DSOGI-PLL is employed in the control strategy of each CPL for the precise extraction of positive and negative sequence voltage components. A CPL control is proposed to achieve the independent compensation of positive and negative sequence of the voltage. The priority has been assigned to the positive sequence voltage control for the maximum FRT enhancement of the SCIG-based wind farm. The positive sequence voltage compensation avoids the acceleration of the rotor and prevents the voltage collapse under severe grid side faults. The negative sequence voltage control is performed to remove the torque oscillation in the SCIG during the asymmetrical fault and it improves the lifetime of the drive train. The incremental current rating of the semiconductor switches of the CPLs is studied and it is observed that the voltage drop, the higher the CPL current rating required for FRT enhancement. The total compensating current injected by the individual CPL belonging to a group of distributed CPLs is compared with the total compensating current by a centralized STATCOM. It is found that each distributed CPL injects less current for FRT enhancement compared to one centralized STATCOM.

REFERENCES

- [1] M. Heydari, A. Y. Varjani, and M. Mohamadian, "A novel variable speed wind energy system using induction generator and six-switch AC/AC converter," in 3rd Power Electronics and Drive Systems Technology (PEDSTC), 2012, pp. 244-250. 602
- [2] A. Bouscayrol, P. Delarue, and X. Guillaud, "Power strategies for maximum control structure of a wind energy conversion system with a synchronous machine," *Renewable Energy*, vol. 30, no. 15, pp. 2273-2288, Dec. 2005.
- [3] S. M. Dehghan, M. Mohamadian, and A. Y. Vm:jani, "A New Variable-Speed Wind Energy Conversion System Using Permanent Magnet Synchronous Generator and Z-Source Inverter," *IEEE Transactions on Energy Conversion*, vol. 24, no. 3, pp. 714-724, Sep. 2009.
- [4] I. A. Baroudi, V. Dinavahi, and A. M. Knight, "A review of power converter topologies for wind generators," in *IEEE International Conference on Electric Machines and Drives*, 2005, pp. 458-465.
- [5] S. Morimoto, H. Kato, M. Sanada, and Y. Takeda, "Output Maximization Control for Wind Generation System with Interior Permanent Magnet Synchronous Generator," in *Conference Record of the IEEE Industry Applications*

Conference Forty-First IAS Annual Meeting, 2006, vol. I, no. C, pp. 503-510.

[6] W.-M. Lin and C.-M. Hong, "Intelligent approach to maximum power point tracking control strategy for variable-speed wind turbine generation system," *Energy*, vol. 35, no. 6, pp. 2440-2447, Jun. 2010.

[7] M. Heydari, A. Yazdian, M. Mohamadian and H. Zahedi, "A Novel Variable-Speed Wind Energy System Using Permanent-Magnet Synchronous Generator and Nine-Switch AC/AC Converter" 1st Power Electronic & Drive System Technologies Conference (PEDSTC), 2010, pp.5 - 9.

[8] M. Heydari, A. Y. Varjani, and M. Mohamadian, "A Novel ThreePhase to Three-Phase AC/AC Converter Using Six IGBTs," in 2nd International Conference on Electric Power and Energy Conversion Systems (EPECS), 2011, UAE.

[9] M. Heydari, A. Yazdi an, M. Mohamadian, and A. Fatemi, "Threephase dual-output six-switch inverter", *IET Power Electronics*, vol.5, pp-1634-1650, 2012.

[10] Raza Kazmi, S.M. ; Goto, H. ; Hai-Jiao Guo; Ichinokura, O. A, "Novel Algorithm for Fast and Efficient Speed-Sen

